Zhen *et al.*
Diabetology & Metabolic Syndrome (2025) 17:57
https://doi.org/10.1186/s13098-025-01578-y

Diabetology &
Metabolic Syndrome

RESEARCH

Open Access

CircRNA-mediated ceRNA regulatory networks: transcriptomic insights into obesity type 2 diabetes progression and treatment strategies

Xian-Jie Zhen[1†], Ren-tong Hu[2†], Nan-Nan Liu[1], Jin-Fang Dou[1], Tao Wu[1], Yue-Lin Zhang[1], Chu-Yue Zhang[1], Li Ma[3*] and Guang-Jian Jiang[1*]

Abstract

The aim of this study was to deeply explore the pathogenesis of obesity type 2 diabetes mellitus (O-T2DM) and search for potential biomarkers through high-throughput RNA sequencing technology. The study included 15 patients with O-T2DM and 15 healthy controls, and peripheral blood samples were collected for transcriptome analysis. The results showed that compared with the control group, there were 442 circRNAs and 2756 mRNAs with significant differential expression in the O-T2DM group. Through weighted gene co-expression network analysis (WGCNA) and pathway enrichment analysis, it was found that the differentially expressed mRNAs were mainly enriched in signaling pathways such as T cell receptor, cell senescence, cytotoxicity mediated by NK cells, IL-17, lipids and atherosclerosis, and the oxidative phosphorylation pathway was activated, and apoptosis was inhibited. Based on the ceRNA theory, a regulatory network was constructed, and key circRNAs such as hsa_circ_0060614 were screened out, which may regulate the expression of the MT2A gene by adsorbing hsa-mir-4668-3p, and the expression levels of the three were significantly increased in O-T2DM patients. This study provides a new perspective for the research on the molecular mechanism of O-T2DM and an important theoretical basis for the development of personalized treatment and precision medicine for it.

Keywords circRNA, qRT-PCR, O-T2DM, ceRNA

Background

Obesity is thought to be a contributing factor to type 2 diabetes and is a common complication in people with type 2 diabetes, significantly associated with an increased risk of T2DM [1–3].Currently, the majority of people with T2DM are overweight or obese [4]. Studies have shown that overweight and obese adults are 2.5 times more likely to develop T2DM than normal-weight individuals [5]. The prevalence of obesity among individuals of childbearing age worldwide has been reported to be as high as 30% [6, 7]. Data from in vitro and in vivo studies indicate that circRNA is a participant in lipogenesis, white fat browning, obesity, obesity-induced

†Xian-Jie Zhen and Ren-tong Hu contributed equally to this work.

*Correspondence:
Li Ma
malixj322122@163.com
Guang-Jian Jiang
bucmjiang@163.com
[1] Diabetes Research Center, School of Traditional Chinese Medicine, Beijing University of Chinese Medicine, Beijing 100029, China
[2] Affiliated Hospital of Youjiang Medical University for Nationalities, Guangxi 533099, China
[3] Traditional Chinese Medicine Hospital Affiliated to Xinjiang Medical University, Wulumuqi 830000, China

inflammation, islet beta cell function, and insulin resistance [8–10].

Non-coding RNA, as a key molecule regulating gene expression, has attracted much attention in recent years [11–13]. CircRNA is a special class of non-coding RNA, which has a circular closed structure and has many functions. It can directly encode proteins [14], derive pseudogenes [15] or combine with genomic DNA to participate in gene transcription regulation [16, 17]. CircRNA can act as competing endogenous RNA (ceRNA), specifically adsorbing miRNA, "isolating" miRNA from target gene mRNA, thus weakening miRNA's negative regulation of mRNA [18]; it can also directly bind to protein to inhibit protein function [17, 19]. CircRNA also plays a role in the pathogenesis of T2DM and T2DM-related complications. Research has indicated that the hsa_circ_0004535/hsa-miR-1827/CASP8 network plays a crucial role in maintaining cell structural integrity and lipid homeostasis [20]. Circular RNA contributes to diabetic foot ulcers, where circHIPK3 promotes cell proliferation, migration, and angiogenesis by up-regulating Nrf2 and VEGFA through down-regulating miR-20b-5p [21]. CircRNA14637 may play a key role in mediating metabolic improvement and adipose mass reduction by regulating fasn and sorbs2 expression via mmu-miR-762 [22]. However, no systematic studies have been reported on circRNA expression patterns in obese diabetes.

The aim of this study was to screen differentially expressed circRNAs and mRNAs in peripheral blood of O-T2DM and healthy subjects by high-throughput sequencing technology, and to analyze their potential biological functions and possible regulatory mechanisms. At the same time, circRNA–miRNA–mRNA regulatory network was constructed according to ceRNA principle to clarify the upstream and downstream regulatory relationship of genes and further reveal the potential function and regulatory mechanism of this network. Through the development of this study, we expect to provide new perspectives and theoretical basis for molecular mechanism research of obesity diabetes and explore new molecular markers and therapeutic targets for the diagnosis and treatment of this disease, thus promoting the development of personalized diagnosis and treatment of T2DM and precision medicine.

Materials and methods

Patient and public involvement

Obesity type 2 diabetes mellitus (O-T2DM) subject selection criteria: (a) all patients met the diagnostic criteria of the American Diabetes Association criteria (2018); (b) fasting blood glucose $\geq$7.0 mmol/L, glycosylated hemoglobin (HbA1C) $\geq$6.5%; (c) body mass index (BMI) $\geq$25 kg/m^2; and (d) patients with complete background information. Exclusion criteria: (a) patients with severe liver, kidney, lung, or systemic disease; (B) patients with malignant tumors; (c) patients with neurological disease; (d) patients with vascular disease, inflammation, and immune disorders. The patients with O-T2DM in this study were from Hepingli Hospital and National Medical Hall of Beijing University of Traditional Chinese Medicine from December 2018 to September 2021, as well as the healthy physical examination population was recruited from the physical examination center of Hepingli Hospital and Water Conservancy Hospital. The study was approved by the Ethics Committee of Beijing University of Traditional Chinese Medicine (BUCM), with the ethical batch number of (2017BZHYLL0105). All procedures were performed in accordance with the Declaration of Helsinki, and all participants received written informed consent. Confidentiality should be observed by both the investigator and the subject. The enrolled subjects were divided into Control and O-T2DM groups (Total = 30, Normal = 15, O-T2DM = 15). There was no statistical difference between the Control and O-T2DM groups in terms of gender and age ($P > 0.05$). After enrollment, fasting venous blood was collected from both groups for subsequent experiments.

Total RNA extraction, mRNA library construction and Illumina sequencing

Peripheral blood was collected from subjects and centrifuged at 12,000×*g* for 15 min at 4 °C to extract serum, total RNA was isolated from collected serum samples using Trizol reagent (Invitrogen, Carlsbad,CA, USA), and RNA concentration and purity (OD260/280 and OD260/230) were measured using NanoPhotometer® spectrophotometer (IMPLEN, CA, USA); The RNA Nano 6000 Assay from Bioanalyzer 2100 Systems (Agilent Technologies, CA, USA) was used to accurately test sample RNA integrity. After RNA purification from total RNA using NEBnext ultra-RNA library prep kit, mRNA was enriched by Oligo (dT) magnetic beads according to manufacturer's instructions. The first strand of cDNA was synthesized in M-MuLV reverse transcriptase system using fragmented mRNA as template and random oligonucleotide as primer. Then the RNA strand was degraded by RNase H, and the second strand of cDNA was synthesized from dNTPs in DNA polymerase I system [23]. The purified double-stranded cDNA was subjected to terminal repair, A-tail addition and sequencing adapter ligation. AMPure XP beads were used to screen cDNA of about 370–420 bp. PCR amplification was performed, and PCR products were purified again by AMPure XP beads. Finally, the library was obtained. The quality of the library was determined by using an Agilent 2100 System (NanoDrop ND-1000) analyzer and accurately quantified

by quantitative real-time polymerase chain reaction (library effective concentrations greater than 2 nM). Prior to data analysis, ribosomal RNA (rRNA) was removed using the Epicentre Ribozero™ rRNA Removal Kit (Epicentre, USA). Linear RNA was removed using RNase R (Epicentre, USA). Subsequently, the fragments were randomly fragmented to 250–300 bp. Through fragment length selection, finally, all RNAs except ribosomal RNA and small-fragment RNAs (such as microRNA, siRNA, etc.) were obtained, including lncRNA, mRNA, circRNA, etc. A strand-specific library was constructed [24], and then sequenced using Illumina NovaSeq 6000.

Data quality control

Sequencing fragments are converted into reads by CASAVA base recognition from image data measured by high-throughput sequencer. Raw data is filtered by removing reads with adapters, removing reads containing N (N indicates that the base information cannot be determined), and removing low-quality reads (reads with Qphred ≤ 20 accounting for more than 50% of the total read length). At the same time, Q20, Q30 and GC content calculations were performed for clean data.

Identification of differentially expressed mRNA and circRNA

The expression of mRNAs was identified by the HTSeq (0.9.1) statistics. The Read Count values on each gene were considered to be the original expression level, and then the Fragments Per Kilobase of transcript sequence per Millions base pairs sequenced (FPKM) method was used to standardize them.

Use the two most commonly-used circRNA identification software, find_circ [19] and CIRI (v2.0.5) [25], and the methods in the corresponding references to identify circRNAs. Meanwhile, use Transcripts Per Kilobase Million (TPM) for normalization of the expression level.

The DESeq2 (version 1.20.0) [26, 27] was used to analyze the differentially expressed mRNAs and circRNAs. RNAs with FC > 1.2 or < 0.833 and pvalue < 0.05 [28] were identified as differentially expressed.

Weighted gene co-expression network analysis

We constructed a co-expression network using WGCNA from the R package [29]. This is a scale-free network construction method that identifies gene clusters with highly correlated expression profiles. By transforming the correlation matrix into an adjacency matrix, we estimate Pearson correlation coefficients among genes according to FPKM values of genes, and then evaluate weighted co-expression relationships among all genes in the adjacency matrix. All genes were clustered by hierarchical clustering and dynamic tree cutting function detection module. To obtain high reliability of the results, the minimum number of genes was set to 30, the sensitivity was set to 3.0, and the module merging threshold was set to 0.25 to generate gene modules. Gene significance (GS) and module membership (MM) are calculated to correlate modules with phenotypic data. MM threshold was set to 0.8 and GS threshold was set to 0.1 to extract the information of corresponding module genes for further analysis [30].

Pathway enrichment analysis

Metascape (https://metascape.org/) database was used to perform pathway enrichment analysis to determine the underlying molecular mechanisms of selected genes. For analysis purposes, we use R to delineate important KEGG pathways according to p-values. Genset enrichment analysis (GSEA) is used to determine whether a defined set of genes shows significant consistent differences between two sample groups. GSEA was performed using GSEA software 2.2.1 (http://www.broadinstitute.org/gsea) [31] and the gene set for C2 was obtained from the molecular signature database v5.2 (http://software.broadinstitute.org/gsea/msigdb).

Construction of circRNA–miRNA–mRNA regulatory network

Certain circRNAs can function as competing endogenous RNAs (ceRNAs) for miRNAs. Candidate circRNAs for constructing circRNA–miRNA–mRNA networks were derived from the differentially expressed circRNAs selected above. RNA Interactomes Encyclopedia of RNA Interactomes (ENCORI, http://starbase.sysu.cn/index.php) was used to predict miRNA binding sites for candidate circRNAs, and these predicted miRNAs constitute candidate miRNAs for circRNA–miRNA–mRNA networks. TargetScan [32], miRDB [33], and miRWalk [34] were then used to predict mRNA targets for candidate miRNAs. The predicted mRNA targets are intersected with the differential mRNAs screened in the above experimental studies to obtain candidate mRNAs of the circRNA–miRNA–mRNA network. Cytoscape software (V3.10.0) was employed to visualize the network, construct the circRNA–miRNA–mRNA network, and conduct data analysis through the application of Network Analyzer and CytoNCA.

Real-time quantitative PCR, RT-qPCR

RT-qPCR was used to verify core RNA expressions in the circRNA–miRNA–mRNA network. Total RNA was extracted from two sample groups and reverse transcribed into cDNA as per the manufacturer's instructions. Reverse transcription for circRNA and mRNA was done using kit No. G3337, while miRNA reverse

transcription employed the A-tail method with kit No. AG11716. CircRNA, mRNA, and miRNA cDNA were prepared following the kit instructions. Amplification was performed on a fluorescence quantitative PCR instrument with the following settings: Stage 1: 95 °C for 30 s; Stage 2 (40 cycles): 95 °C for 20 s, 60 °C for 30 s; Stage 3 (melting curve): 65 °C to 95 °C. Fluorescence signals were collected every 0.5 °C. CT values were obtained at the end of the cycle. β-actin served as the internal reference for circRNA and mRNA, while U6 was used for miRNA. Relative expression levels were calculated using the $2-\triangle\triangle Ct$ method (primer sequences in Table 1).

Statistical methods

SPSS 20.0 (SPSS, Inc., Chicago, IL, USA) software, and the measurement data were expressed as x ± s. The measurement data that met the normality were analyzed for significant differences using one-way analysis of variance, and the measurement data that did not meet the normality were analyzed for significant differences using the Kruskal Wallis nonparametric test. The Chi-square test was used for frequency distribution data. $P<0.05$ was considered statistically significant.

Results

Clinical characteristics of subjects

Our study enrolled 15 patients with O-T2DM and 15 healthy people. All patients with O-T2DM met the diagnostic criteria of fasting plasma glucose (FPG) ≥ 7.0 mmol/L, glycosylated hemoglobin (HbA1C) ≥ 6.5%, and BMI ≥ 25 kg/m^2. As shown in Table 2, FPG, HbA1c, TG levels and BMI index were significantly increased, and HDL-C level was significantly decreased in the O-T2DM group compared with the Control group ($P<0.01$). There were significant differences in mean BMI between the two groups ($P>0.005$).

Table 1 Primer sequences

Gene	Primer sequences
β-actin	F: GTGGCCGAGGACTTTGATTG
	R: CCTGTAACAACGCATCTCATATT
hsa_circ_0060614	F: TTCAGTGCGAGCGAGGAGTC
	R: TGTTGCTCCATGTCTAATCATTTGA
MT2A	F: CAAAGGGGCGTCGGACAAGTG
	R: CAAACGGTCACGGTCAGGGTTG
U6	F: CTCGCTTCGGCAGCACA
	R: AACGCTTCACGAATTTGCGT
hsa-mir-4668- 3p	F: GGGAAAATCCTTTTTGTTTTTCCAG
	R: Kit (AG11716)

F forward, *R* reverse

Table 2 Basic information and biochemical indicators of subjects ($x \pm s$, n = 15)

	Control	O-T2DM
Gender (M/F)	8/7	7/8
Age (year)	54.60 ± 9.42	53.67 ± 7.23
FPG (mmol/L)	5.38 ± 0.65	11.97 ± 4.51***
HbA1c (%)	5.67 ± 0.21	8.54 ± 1.77***
BMI (kg/m^2)	23.44 ± 2.67	27.07 ± 1.51***
TC (mmol/L)	5.21 ± 0.94	5.37 ± 1.08
TG (mmol/L)	1.28 ± 0.66	3.11 ± 2.61**
LDL-C (mmol/L)	2.91 ± 1.02	3.18 ± 0.77
HDL-C (mmol/L)	1.64 ± 0.47	1.12 ± 0.4**

FPG fasting plasma glucose, *HbA1c* glycosylated hemoglobin, *BMI* body mass index, *TC* total cholesterol, *TG* triglyceride, *LDL-C* low density lipoprotein, *HDL-C* high density lipoprotein

*: $P<0.05$, **: $P<0.01$, ***: $P<0.001$ compared with Control group

Quality assessment and mapping results

To construct mRNA and circRNA expression profiles for O-T2DM and Control, transcriptome datasets were generated by RNA-seq. Sequencing outputs were then subjected to quality control and mapping analysis (Supplementary Table 1). Q20 (representing the probability of correct base detection) > 93%, Q30 > 85%, the overall sequencing error rate is below 0.04%. These results may indicate that transcriptome sequencing data has appropriate mapping quality.

Differentially expressed mRNA and circRNA

Sequencing technology was used to detect differentially expressed mRNA and circRNA in peripheral blood between Control group and O-T2DM group. As shown in Fig. 1B, O-T2DM_VS_Control detected a total of 2756 differentially expressed mRNAs. As shown in Fig. 1C, 442 differentially expressed circRNAs were detected (FC > 1.2 or FC < 0.833, P < 0.05). Figure 1D–H is weighted gene co-expression network analysis (WGCNA) of mRNA. Analysis of the relationship between modules and clinical characteristics found that white (cor = ± 0.74, P < 0.001), lightsteelblue1 (cor = ± 0.48, P < 0.001) and darkmagenta (cor = ± 0.44, P = 0.01) were significantly correlated with phenotypes. Then the absolute value of correlation threshold was set to > 0.8, and the Hub genes in two modules were extracted regardless of phenotype for enrichment analysis.

Pathway enrichment analysis

The modules significantly correlated with phenotypes were screened from mRNA WGCNA results, and KEGG enrichment analysis was performed on Hub genes extracted from the modules. As shown in Fig. 2A, B,

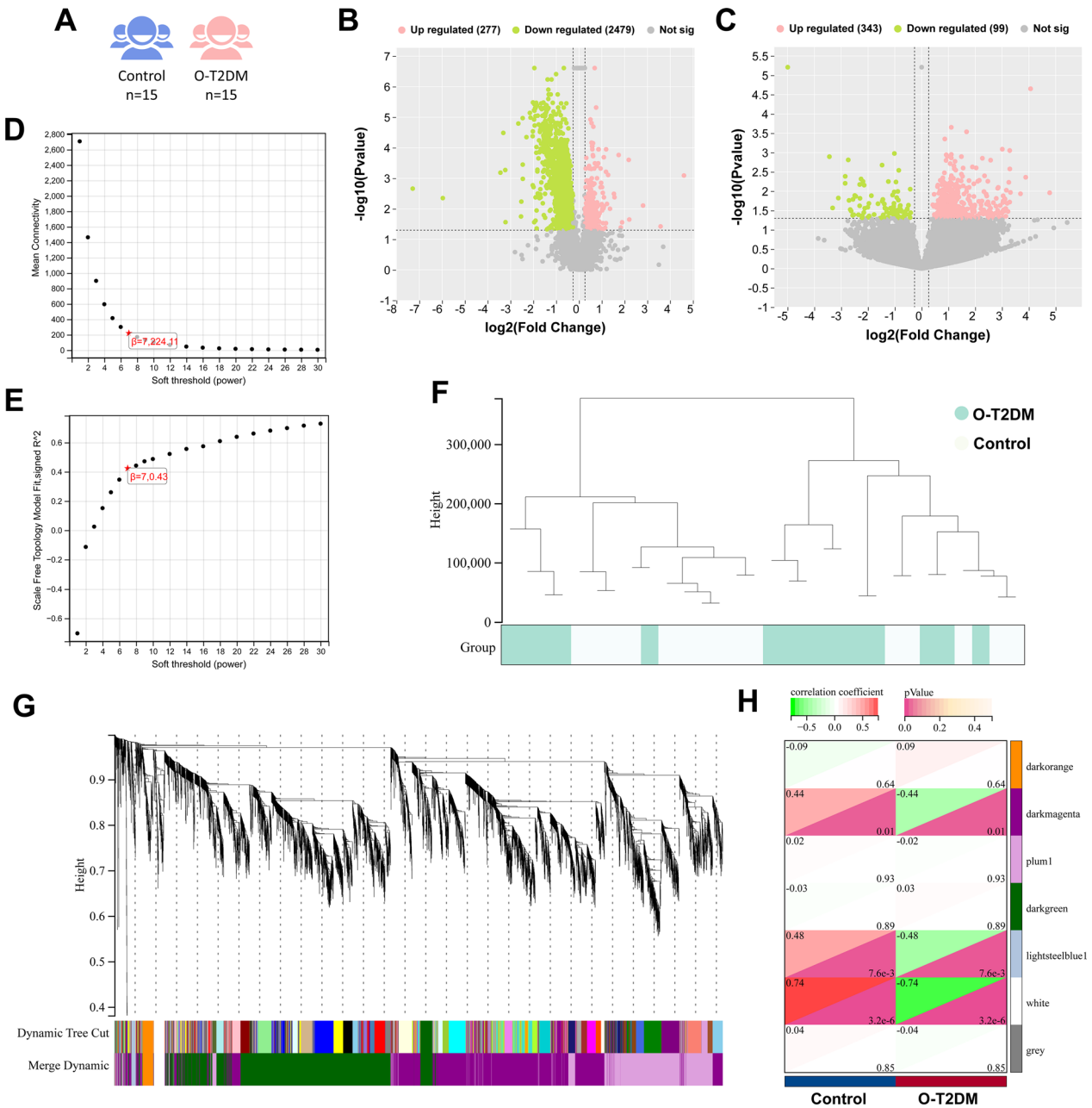

Fig. 1 Transcriptomic analysis of serum from subjects. **A** The schematic diagram depicts the recruitment of both normal individuals and O-T2DM patients. **B**, **C** Visual statistical results of differential gene analysis. Volcano plots of mRNA (**B**), circRNA (**C**) expression. Each dot in the graph represents a specific gene or transcript; the red dots represent significantly upregulated genes; the green dots represent significantly downregulated genes, and the gray dots represent genes without significantly different expression. **D** The relationship between the mean connectivity and various soft-thresholding powers. **E** The relationship between the scale-free fit index and various soft-thresholding powers. **F** Clustering dendrogram of 30 samples. **G** The cluster dendrogram was constructed using WGCNA based on topological overlap dissimilarity, with each distinct color denoting a particular gene co-expression module. **H** Heat map of the correlation between each color module and phenotype

the enrichment results of darkmagenta and lightsteelblue1 modules are respectively shown. Enriched in T cell receptor, cellular senescence, natural killer cell mediated cytotoxicity, IL-17, lipids and atherosclerosis signaling pathways. GSEA analysis of differential mRNA showed that oxidative phosphorylation pathway was activated in O-T2DM group, whereas apoptosis was inhibited in O-T2DM group (Fig. 2C, D).

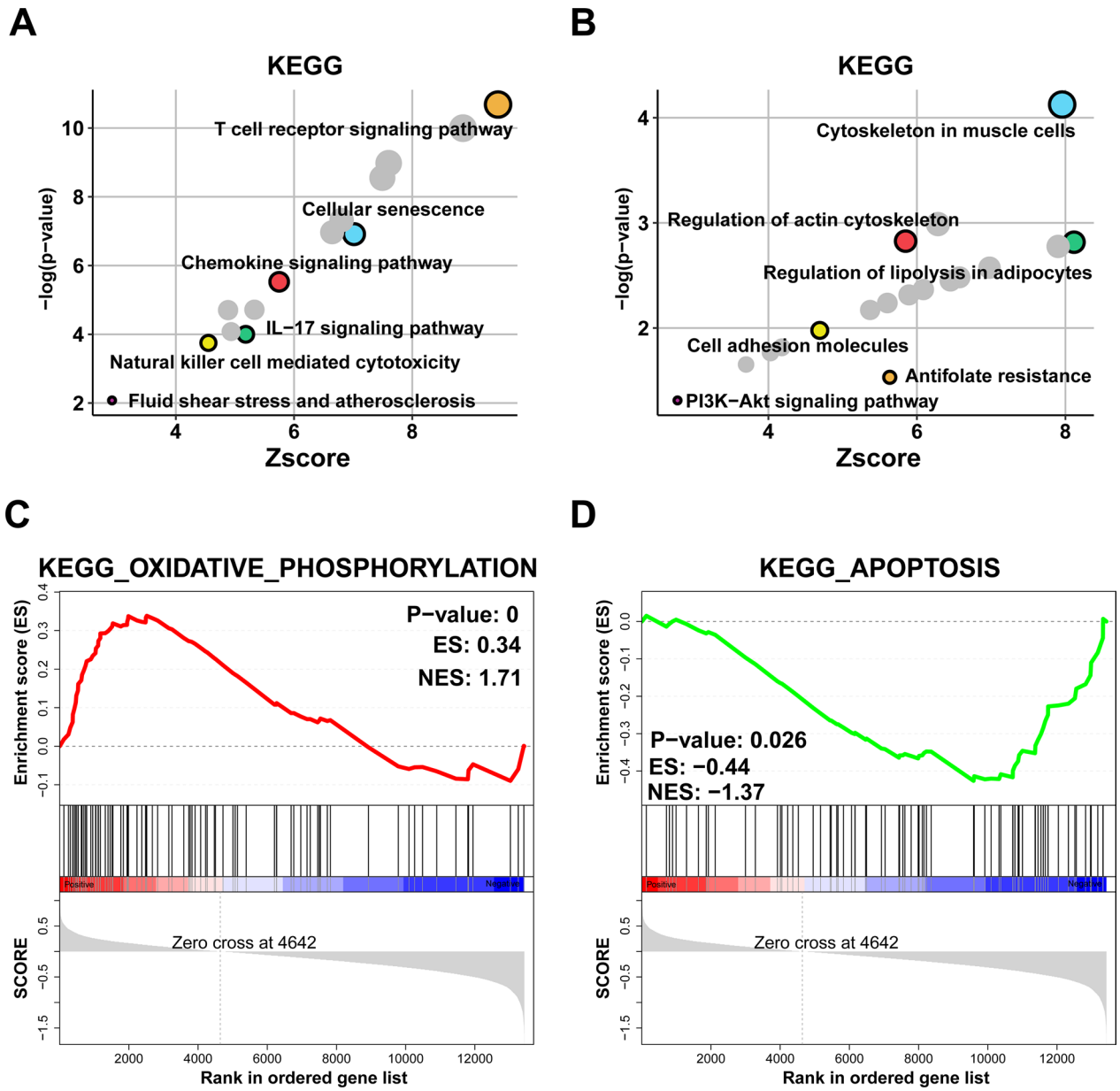

Fig. 2 Enrichment analysis results of gene modules. **A** KEGG pathways of the hub genes in the darkmagenta module are plotted according to the adjusted p-value (y-axis) and the non-statistical Z-score calculated by GoPlot (x-axis). The area of each circle represents the number of genes of that pathway. **B** KEGG pathways of the hub genes in the lightsteelblue1 module. **C**, **D** GSEA of oxidative phosphorylation (**C**) and apoptosis (**D**) pathways between control and O-T2DM groups. There is a scale panel below, with black vertical lines representing significant genes. The left side (red) represents genes that are upregulated in the O-T2DM group compared to the control group, while the right side (blue) represents genes that are downregulated

Construction of circRNA–miRNA–mRNA network

We used miRanda software to predict miRNA binding sites differentially expressed in circRNA between O-T2DM and Control groups. The results showed that 264 of the 442 differential circRNAs predicted miRNA binding sites, involving a totally of 2643 different miRNAs as miRNA candidates.

TargetScan, miRDB and miRWalk databases were used to identify 6991 mRNA targets. Intersecting the predicted candidate mRNAs with the 2756 differentially expressed mRNA screened by sequencing yielded 1281 candidate mRNAs (Fig. 3).

264 differential circRNAs, 2643 candidate miRNAs and 1281 candidate mRNAs were introduced into

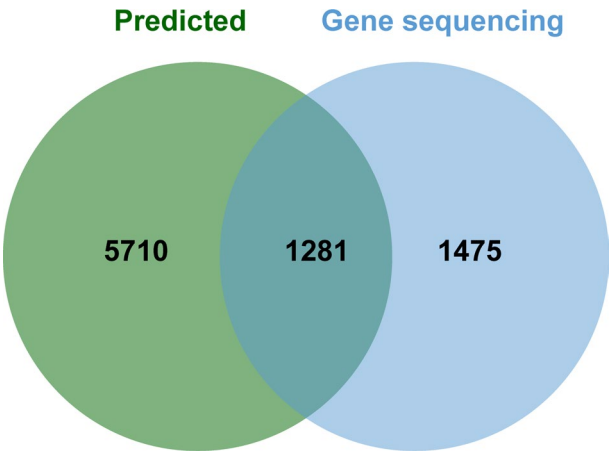

Fig. 3 Intersection of the differentially expressed mRNAs and database-predicted mRNAs

cytoscape to construct circRNA-miRNA-mRNA regulatory network map of O-T2DM and Control groups, and circRNA, miRNA and mRNA that did not conform to ceRNA competition principle were deleted. The circRNA-miRNA-mRNA network includes 4209 nodes and 135,344 edges, involving 264 circRNAs, 1789 miRNAs and 1281 mRNAs.

Only the top 5 circRNAs with differential expression multiples among 264 circRNAs were retained to construct the ceRNA network regulated by them, as shown in Fig. 4A. The ceRNA network in which the top 5 circRNAs are involved consists of 78 nodes and 125 edges in total. The 22 kinds of mRNAs involved in the ceRNA network are mainly enriched in endocrine resistance, inflammatory mediator regulation of TRP channels, TNF, cellular senescence, rap1, MAPK, mineral absorption and insulin secretion (Fig. 4B). MT2A was the most differentially expressed mRNA in the network (FC = 1.74, P = 0.0086). Sponge hsa_circ_0060614 combined with hsa-mir-4668- 3p promotes MT2A expression.

hsa_circ_0060614 functions via the ceRNA network axis of hsa-mir-4668-3p/MT2A

We constructed a ceRNA network to identify the hsa_circ_0060614/hsa-mir-4668-3p/MT2A pathway. Sequencing revealed significant increases in hsa_circ_0060614 and MT2A expression. To confirm the targets, we analyzed RNA from O-T2DM and healthy controls using qRT-PCR for MT2A, hsa-mir-4668-3p, and hsa_circ_0060614. Results showed elevated levels of these markers in O-T2DM patients' blood (Fig. 5A–C).

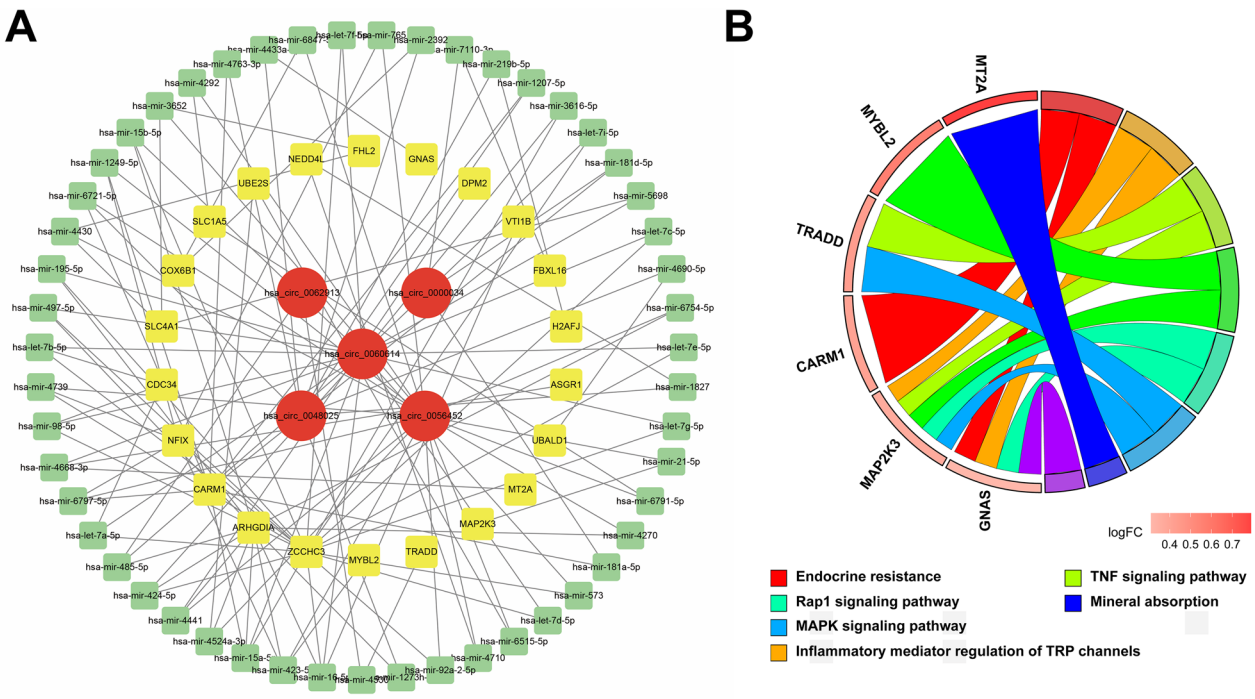

Fig. 4 Construction of ceRNA network map and KEGG enrichment analysis of mRNAs involved. **A** CircRNA–miRNA–mRNA regulatory network constructed based on the mechanism of action of ceRNAs. Note: Green squares: miRNA; yellow squares: mRNA; red circles: circRNA. **B** Chord plots show the relationship between mRNAs and the KEGG pathway

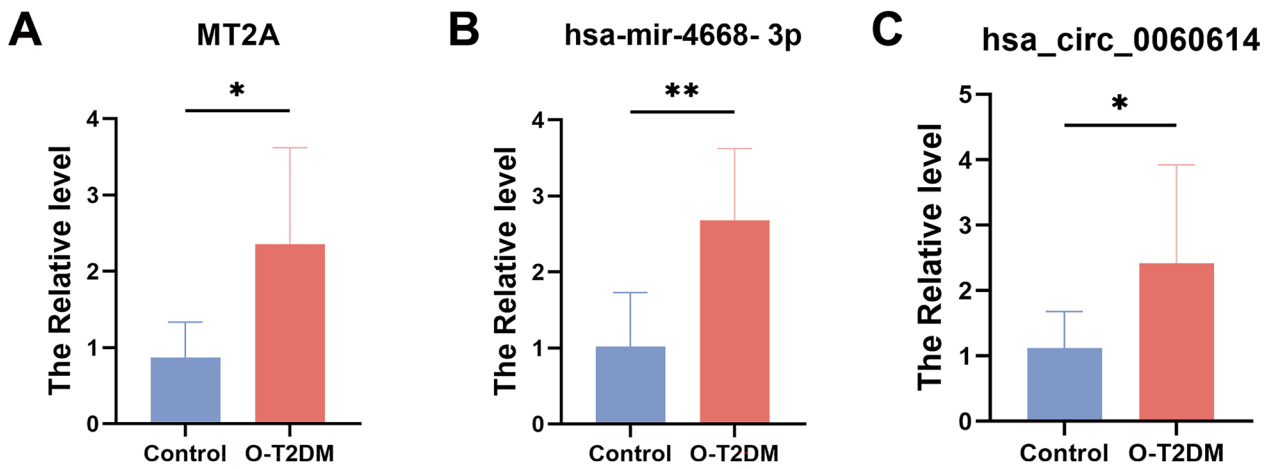

Fig. 5 The relative expression level of DEGs involved in the ceRNA network detected by RT-qPCR. Data are presented as mean ± SD. *$p < 0.05$, *$p < 0.01$, ***$p < 0.001$, and ****$p < 0.0001$ compared between groups, based on independent samples t-test

Discussion

Obesity represents a significant risk factor for T2DM, with a close association between the two. The likelihood of developing T2DM is notably elevated in obese individuals, and the majority of T2DM patients are accompanied by overweight or obesity issues. Previous investigations have demonstrated that circRNA is involved in various processes, including adipogenesis [35, 36], obesity [37, 38], obesity-related inflammation [39, 40], islet β-cell function [8], and insulin resistance [41]. Nevertheless, research focusing on exploring the pathogenesis of obesity and diabetes from the perspective of circRNA remains insufficient.

This research conducted an analysis of the peripheral blood of O-T2DM patients and healthy individuals through high-throughput sequencing technology and established a circRNA–miRNA–mRNA regulatory network. The WGCNA revealed that the differentially expressed mRNAs were concentrated in signal pathways such as the T cell receptor, cell senescence, cytotoxicity mediated by NK cells, IL-17, lipid, and atherosclerosis. The GSEA demonstrated that the oxidative phosphorylation pathway was activated, and apoptosis was inhibited in the O-T2DM group. These results are in line with previous research findings. For instance, a review study by Theresa V Rohm et al. indicated that the obesity-related inflammatory signaling pathway is of great significance in the pathogenesis of diabetes [42], and the inflammatory-related pathways involved in this study further corroborate this perspective.

This study identified key circRNAs like hsa_circ_0060614, which might modulate the expression of the MT2A gene by adsorbing hsa-mir-4668-3p, and the expressions of all three were markedly elevated in O-T2DM patients. The MT2A gene is associated with the risk of diabetes, and its expression is augmented in the adipose tissue of obese type 2 diabetes patients. It is also intimately related to diverse biological processes, including inflammation, the MAPK signaling pathway, cell senescence, cytotoxicity, mineral absorption, and oxidative stress. This is in accordance with the significance of MT2A in diabetes-related metabolic disorders as discovered in other studies. For instance, the elevation of pro-inflammatory chemokines in patients with atherosclerosis is closely tied to the abnormal expression of MT2A. Under inflammatory stimulation, the up-regulation of MT2A expression can bolster the antioxidant ability, yet it can also alter the metal homeostasis, exacerbate atherosclerosis, and trigger cytotoxicity and death. Inhibiting inflammation and maintaining MT homeostasis are beneficial for ameliorating T2DM [43–45].

Conclusion

For the first time, this article has conducted a systematic study on O-T2DM from the perspective of the ceRNA regulatory network mediated by circRNA, thereby providing a novel explanatory dimension for its pathogenesis and highlighting the crucial role of circRNA in modulating mRNA expression and consequently influencing disease progression. Based on the ceRNA theory, a regulatory network was established, and molecules including hsa_circ_0060614, hsa-mir-4668-3p and MT2A were identified as potential biomarkers for O-T2DM. MT2A is intimately associated with inflammation, MAPK, cell senescence, cytotoxicity, mineral absorption, oxidative stress, and the like. Moreover, its abnormal expression plays a pivotal role in the development of the disease, furnishing a theoretical foundation

for the development of personalized treatment strategies and precision medicine for this ailment.

Limitations of this study

1. Although the circRNA–miRNA–mRNA regulatory network has been constructed, most of it is based on bioinformatics prediction and analysis. Future studies should conduct in vitro and in vivo functional verification experiments, such as cell transfection experiments, gene knockout/overexpression experiments, and animal model experiments, to deeply explore the specific biological functions and regulatory mechanisms of key circRNAs, miRNAs, and mRNAs in the pathogenesis of O-T2DM, and further clarify the causal relationship.
2. The current study is deficient in validation using external data. Validating the identified genes using microarray or RNA-seq datasets from GEO can significantly enhance the reliability of the findings [46, 47].

Suggestion

In light of the potential targets unearthed in this study, it is possible to conduct relevant investigations in the realm of drug research and development. By screening small molecule compounds, biological agents, and the like that are capable of modulating the expression of crucial circRNAs, miRNAs, or mRNAs, new drug candidates and treatment strategies for the treatment of O-T2DM can be furnished.

Supplementary Information

The online version contains supplementary material available at https://doi.org/10.1186/s13098-025-01578-y.

Supplementary Material 1.

Acknowledgements
Not applicable.

Author contributions
Jiang and ma have made substantial contributions to the conception; zhen and hu have drafted the work or substantively revised it; liu and dou have made the acquisition, analysis; wu, zhang and zhang have made interpretation of data, all authors reviewed the manuscript.

Funding
This work was supported by Key Research and Development Project of Xinjiang Uygur Autonomous Region, China (2023B03002), the Incubation Project for Major Scientific Research Programs of Xinjiang Medical University (XYD2024ZX06), and the National Natural Science Foundation of China (82260931).

Availability of data and materials
The datasets used and analyzed during the current study are available from GEO (GSE278204).

Declarations

Ethics approval and consent to participate
The study was approved by the Ethics Committee of Beijing University of Traditional Chinese Medicine (BUCM), with the ethical batch number of (2017BZHYLL0105). All procedures were performed in accordance with the Declaration of Helsinki, and all participants received written informed consent.

Consent for publication
Both written and verbal consent was obtained from the subjects of the study.

Competing interests
The authors declare no competing interests.

Received: 28 September 2024 Accepted: 3 January 2025
Published online: 14 February 2025

References

1. Smith KB, Smith MS. Obesity statistics. Prim Care. 2016; 43(1): 121–35, ix.
2. Arroyo-Johnson C, Mincey KD. Obesity epidemiology worldwide. Gastroenterol Clin North Am. 2016;45(4):571–9.
3. DeFronzo RA, et al. Type 2 diabetes mellitus. Nat Rev Dis Primers. 2015;1:15019.
4. Classification and Diagnosis of Diabetes. Standards of medical care in diabetes-2021. Diabetes Care. 2021;44(Suppl 1):S15-s33.
5. Wang C, et al. Type 2 diabetes mellitus incidence in Chinese: contributions of overweight and obesity. Diabetes Res Clin Pract. 2015;107(3):424–32.
6. Grzegorczyk-Martin V, et al. IVF outcomes in patients with a history of bariatric surgery: a multicenter retrospective cohort study. Hum Reprod. 2020;35(12):2755–62.
7. Ogunwole SM, Zera CA, Stanford FC. Obesity management in women of reproductive age. JAMA. 2021;325(5):433–4.
8. Liu Y, et al. Circular RNA circGlis3 protects against islet β-cell dysfunction and apoptosis in obesity. Nat Commun. 2023;14(1):351.
9. Liu Y, et al. Circular RNA SAMD4A controls adipogenesis in obesity through the miR-138-5p/EZH2 axis. Theranostics. 2020;10(10):4705–19.
10. Chen Z, et al. Myeloid cell TRAF3 promotes metabolic inflammation, insulin resistance, and hepatic steatosis in obesity. Am J Physiol Endocrinol Metab. 2015;308(6):E460–9.
11. Matsui M, Corey DR. Non-coding RNAs as drug targets. Nat Rev Drug Discov. 2017;16(3):167–79.
12. Ren B, et al. Emerging functions of mitochondria-encoded noncoding RNAs. Trends Genet. 2023;39(2):125–39.
13. Zong Y, et al. Decoding the regulatory roles of non-coding RNAs in cellular metabolism and disease. Mol Ther. 2023;31(6):1562–76.
14. Chen R, et al. Engineering circular RNA for enhanced protein production. Nat Biotechnol. 2023;41(2):262–72.
15. Liu J, et al. Circles reshaping the RNA world: from waste to treasure. Mol Cancer. 2017;16(1):58.
16. Conn VM, et al. A circRNA from SEPALLATA3 regulates splicing of its cognate mRNA through R-loop formation. Nat Plants. 2017;3:17053.
17. Hansen TB, et al. miRNA-dependent gene silencing involving Ago2-mediated cleavage of a circular antisense RNA. Embo j. 2011;30(21):4414–22.
18. Hansen TB, et al. Natural RNA circles function as efficient microRNA sponges. Nature. 2013;495(7441):384–8.
19. Memczak S, et al. Circular RNAs are a large class of animal RNAs with regulatory potency. Nature. 2013;495(7441):333–8.
20. Li M, et al. Circ_0004535/miR-1827/CASP8 network involved in type 2 diabetes mellitus with nonalcoholic fatty liver disease. Sci Rep. 2023;13(1):19807.

21. Liang ZH, et al. UCMSCs-derived exosomal circHIPK3 promotes ulcer wound angiogenesis of diabetes mellitus via miR-20b-5p/Nrf2/VEGFA axis. Diabet Med. 2023;40(2): e14968.
22. Zhao Q, et al. Duodenal-Jejunal bypass improves metabolism and re-models extra cellular matrix through modulating ceRNA network. Genomics. 2023;115(6): 110744.
23. Amirmahani F, et al. Approaches for the integration of big data in translational medicine: single-cell and computational methods. Ann N Y Acad Sci. 2021;1493(1):3–28.
24. Parkhomchuk D, et al. Transcriptome analysis by strand-specific sequencing of complementary DNA. Nucleic Acids Res. 2009;37(18): e123.
25. Gao Y, Wang J, Zhao F. CIRI: an efficient and unbiased algorithm for de novo circular RNA identification. Genome Biol. 2015;16(1):4.
26. Love MI, Huber W, Anders S. Moderated estimation of fold change and dispersion for RNA-seq data with DESeq2. Genome Biol. 2014;15(12):550.
27. Gholami D, et al. MiR-182-5p, MiR-192-5p, and MiR-493-5p constitute a regulatory network with crisp3 in seminal plasma fluid of teratozoospermia patients. Reprod Sci. 2021;28(7):2060–9.
28. Wang J, et al. Exosomal PD-L1 and N-cadherin predict pulmonary metastasis progression for osteosarcoma patients. J Nanobiotechnol. 2020;18(1):151.
29. Langfelder P, Horvath S. WGCNA: an R package for weighted correlation network analysis. BMC Bioinform. 2008;9:559.
30. Heidarzadehpilehrood R, et al. Weighted gene co-expression network analysis (WGCNA) discovered novel long non-coding RNAs for polycystic ovary syndrome. Biomedicines. 2023;11(2):518.
31. Grover A, et al. Single-cell RNA sequencing reveals molecular and functional platelet bias of aged haematopoietic stem cells. Nat Commun. 2016;7:11075.
32. Agarwal V, et al. Predicting effective microRNA target sites in mammalian mRNAs. Elife. 2015;4: e05005.
33. Chen Y, Wang X. miRDB: an online database for prediction of functional microRNA targets. Nucleic Acids Res. 2020;48(D1):D127-d131.
34. Dweep H, et al. miRWalk–database: prediction of possible miRNA binding sites by "walking" the genes of three genomes. J Biomed Inform. 2011;44(5):839–47.
35. Li J, et al. A nanodrug system overexpressed circRNA_0001805 alleviates nonalcoholic fatty liver disease via miR-106a-5p/miR-320a and ABCA1/CPT1 axis. J Nanobiotechnol. 2021;19(1):363.
36. Chen X, et al. Circ_0057558 promotes nonalcoholic fatty liver disease by regulating ROCK1/AMPK signaling through targeting miR-206. Cell Death Dis. 2021;12(9):809.
37. Zaiou M. The emerging role and promise of circular RNAs in obesity and related metabolic disorders. Cells. 2020;9(6):1473.
38. Zhang Y, et al. Emerging functions of circular RNA in the regulation of adipocyte metabolism and obesity. Cell Death Discov. 2022;8(1):268.
39. Marques-Rocha JL, et al. Noncoding RNAs, cytokines, and inflammation-related diseases. Faseb j. 2015;29(9):3595–611.
40. Li G, et al. Transcriptome of visceral adipose tissue identifies an inflammation-related ceRNA network that regulates obesity. Mol Cell Biochem. 2022;477(4):1095–106.
41. Lin X, et al. CircRNF111 protects against insulin resistance and lipid deposition via regulating miR-143-3p/IGF2R axis in metabolic syndrome. Front Cell Dev Biol. 2021;9: 663148.
42. Rohm TV, et al. Inflammation in obesity, diabetes, and related disorders. Immunity. 2022;55(1):31–55.
43. Giacconi R, et al. Novel -209A/G MT2A polymorphism in old patients with type 2 diabetes and atherosclerosis: relationship with inflammation (IL-6) and zinc. Biogerontology. 2005;6(6):407–13.
44. Giacconi R, et al. The +838 C/G MT2A polymorphism, metals, and the inflammatory/immune response in carotid artery stenosis in elderly people. Mol Med. 2007;13(7–8):388–95.
45. Zhang X, et al. Long-term 4-nonylphenol exposure drives cervical cell malignancy through MAPK-mediated ferroptosis inhibition. J Hazard Mater. 2024;471: 134371.
46. Rahimpour A, et al. A comprehensive bioinformatic analysis revealed novel MicroRNA biomarkers of Parkinson's disease. Cell Biol Int. 2022;46(11):1841–51.
47. Rahimpour A, et al. Bioinformatics analysis of MicroRNA profiles unveils novel biological markers of Alzheimer's disease. Neurochem J. 2022;16(3):334–42.

Publisher's Note